# Accepted Manuscript

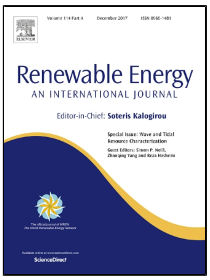


Effects of Contamination and Erosion at the Leading Edge of Blade Tip Airfoils on the Annual Energy Production of Wind Turbines

Woobeom Han, Jonghwa Kim, Bumsuk Kim

| | |
|---|---|
| PII: | S0960-1481(17)30864-9 |
| DOI: | 10.1016/j.renene.2017.09.002 |
| Reference: | RENE 9200 |
| To appear in: | *Renewable Energy* |
| Received Date: | 27 July 2016 |
| Revised Date: | 02 May 2017 |
| Accepted Date: | 02 September 2017 |

Please cite this article as: Woobeom Han, Jonghwa Kim, Bumsuk Kim, Effects of Contamination and Erosion at the Leading Edge of Blade Tip Airfoils on the Annual Energy Production of Wind Turbines, *Renewable Energy* (2017), doi: 10.1016/j.renene.2017.09.002

# Highlights

- **The effects of leading edge damage on the performance of wind turbines were examined.**
- **The L.E damage reduces the aerodynamic coefficients and the power output of the blade.**
- **Contamination and erosion conditions reduced AEP by 2%–3.7%.**

# Effects of Contamination and Erosion at the Leading Edge of Blade Tip Airfoils on the Annual Energy Production of Wind Turbines

Woobeom Han, Jonghwa Kim, Bumsuk Kim*

*Corresponding author: Bumsuk Kim

Faculty of Wind Energy Engineering, Jeju National Universty, Republic of Korea

Tel/Fax: +82-64-754-4402/+82-64-702-2479

E-Mail: bkim@jejunu.ac.kr

**Abstract:** Contamination and erosion at the leading edge of blade tips adversely affect the annual energy production (AEP) of wind turbines. Obtaining pertinent quantitative data would help in the efficient planning of operations and maintenance of these turbines. In this study, to quantitatively analyze the effects of contamination and erosion on the aerodynamic performance of a blade tip airfoil (NACA 64-618) and in turn on the AEP loss of wind turbines, transient computational fluid dynamics simulations and AEP calculations were performed for a 5-MW National Renewable Energy Laboratory wind turbine. The simulations indicated that depending on the severity of the conditions, contamination and erosion conditions reduced and increased the lift and drag coefficients, respectively, of the blade by up to 53% and 314%. Contamination and erosion conditions reduced AEP by 2%–3.7%.

**Keywords:** annual energy production; computational fluid dynamics; equivalent sand grain roughness; NACA64618; NREL 5-MW reference wind turbine; lift coefficient; drag coefficient; erosion; contamination

## 1. Introduction

Contaminant accumulation and erosion can occur at the leading edge of wind turbine blades that have been in operation for a long period because of various environmental conditions, such as dust, rain, and hail; thus, these blades require regular inspection and maintenance. The extent of contamination and erosion depends on the temperature, humidity, presence of contaminants in the atmosphere, and wind speed. The installation and operational conditions significantly affect the power and load variation of wind turbines [1].

The leading edge of blades of wind turbines operating in wind farms have been reported to have high rates of contamination and damage due to erosion [2]. Atmospheric particles, raindrops, and hail impacting the wind turbine blades rotating at high speeds is the primary cause of surface erosion at the leading edges of these blades; such impacts change the shape and surface roughness of the leading edge. Initially, small, irregularly distributed pits form on the pressure side of the blade and near the stagnation

point; these pits gradually develop into gouges as the pits combine. Further erosion can lead to complete removal of the coating layer on the blade surface, thus exposing the shell laminate. In severe cases, delamination—cracking at the junction of the leading edge—occurs, significantly affecting the structural stability of the blade.

Erosion density is high near the leading edge of blades and decreases in the chordwise direction [3] because contaminant accumulation and erosion typically begin from the leading edge, which is exposed to high wind speeds; thus, such accumulation and erosion significantly affect the power performance and load variation of wind turbines.

Khalfallah and Koliub analyzed the effects of dust particle contamination at the leading edge of wind turbine blades on the output power performance of a 300-kW wind turbine installed in a desert and reported that dust accumulation tends to occur at the stagnation point of the leading edge. In addition, they proposed a formula for calculating the reduction in the output power according to the height and area of the contaminated section [4]. Corten and Veldkamp et al. have reported that contamination due to insects mainly occurs in regions with low wind speeds, temperatures of 10°C and higher, and low humidity, which are favorable conditions for insects. Moreover, they confirmed that the output power decreases by up to 25% when the wind speed is higher than the rated wind speed [5-6].

Persistent contaminant accumulation and erosion (Fig. 1) on the surface of the wind turbine blades can induce premature transition and turbulence, which in turn induces early flow separation, directly increasing the power losses and fatigue load of wind turbines. An inspection of 201 blades of 67 wind turbines operated by EDP Renováveis revealed erosion at the leading edge of 174 blades (87%) and contamination due to dirt and grease on 197 blades (98%) [2]. Vestas measured the power performance of 1.5-MW active-stall wind turbines with various levels of contamination at the leading edge of blades and reported that extreme contamination reduces annual energy production (AEP) by 10%–13% [7].

In addition to the aforementioned studies, several studies have examined the correlation between contamination and erosion at the leading edge of blades with wind turbine AEP loss and operation and maintenance (O&M) costs through wind tunnel tests and numerical simulations. For example, Ren et al. [8-9] and Li et al. [9] have examined, through two-dimensional computational fluid dynamics (CFD) simulations, the effects of contaminant accumulation at the leading edge of airfoils on their aerodynamic performance and have proposed the critical conditions of roughness area and height. However, these studies have considered few angles of attack (specifically 2° and 10.7°), and data on the aerodynamic performance of airfoils at various angles of attack are lacking; this data could be used to estimate the effects of aerodynamic performance on AEP loss and load variation of wind turbines.

Sareen et al. (2014) examined the effects of different stages of erosion (i.e., pits, gauges, and delamination) on the airfoils (DU96-W-180) of wind turbines through 2D airfoil wind tunnel tests for flows with Reynolds numbers of 1.00 × E06, 1.50 × E06, and 1.85 × E06 [3]. However, the Reynolds number at the cross-section of blade tip airfoils of large wind turbines vary according to the operational conditions and exceeds 6.00 × E06 at rated wind speeds. Blade contamination and erosion on the blades of large wind turbines occur mainly at the leading edge, which are exposed to winds with high angular

velocity. However, no data is available regarding the AEP loss of large wind turbines at high Reynolds number flows. Further, to protect wind turbines from contamination and erosion, systematic inspection and O&M plans that consider blade surface conditions should be implemented, but O&M in most wind farms is inefficient because quantitative data on the effects of contaminant accumulation and erosion on the power performance and load variation of wind turbines are lacking. Thus, this study quantitatively analyzed the aerodynamic performance of blade tip airfoils exposed to various contamination and erosion conditions in large wind turbines through transient CFD simulations and calculated the corresponding AEP losses through integrated load calculations.

## 2. Wind Turbine Model and Blade Damage Conditions

### *2.1 Wind turbine model*

In this study, design information of 5-MW National Renewable Energy Laboratory (NREL) wind turbine [10] was used to analyze the aerodynamic performance of wind turbines, in terms of AEP loss, with variation in the contamination and erosion conditions at the blade airfoil. The rated wind speed and rotor speed of the 5-MW NREL wind turbine are 11.4 m/s and 12.1 rpm, respectively. The rotor diameter and hub height are 126 and 90 m, respectively. The diameter and thickness of the tower bottom, fabricated from structural steel, are 6 and 0.027 m, and those of the tower top are 3.87 and 0.016 m, respectively. The variable speed control maximizes the output power performance at lower-than-rated wind speeds, whereas the variable blade pitch control stabilizes the output at higher-than-rated wind speeds. Detailed specifications of this wind turbine are presented in Table 1.

### *2.2 Airfoil for CFD simulations*

In the design process of wind turbine blades, the type and thickness distribution of airfoils located at various radial distances are determined by considering power performance, structural stability, and operational conditions. Specifically, thin airfoils, which exhibit excellent aerodynamic performance, are placed in the blade tip area to maximize the output power performance.

Kerho et al. [11] investigated the correlation between Reynolds number and the surface boundary layer of NACA0012 airfoils with variation in the height and area of contaminant accumulation at the leading edge. The results showed that changes in the internal flow of the boundary layer of airfoils are larger for flows with higher Reynolds number. In addition, higher Reynolds number flows exert stronger effects even under light contamination conditions. For example, significant output power losses can occur at low contamination or erosion levels at the leading edge of blades of large wind turbines because at the rated wind speeds, the wind speed at the airfoils tends to be 60–80 m/s. Therefore, a NACA64-618 airfoil located at the tip of an NREL 5-MW wind turbine was considered in the CFD simulation.

### *2.3 Blade contamination and erosion conditions*

Usually, aerodynamic performance of the leading edge of wind turbine blades reduces as the height and area of the surface roughness increase; however, this relationship is not always linear. Li et al. reported that when the roughness height is 0.3 mm and roughness area exceeds 50%, a fully turbulent boundary layer is formed as the roughness area on the suction side of the airfoil increases, thereby reducing the reduction in aerodynamic performance.

Khalfallah and Koliub showed that the height of the surface roughness at the leading edge of a blade of a wind turbine installed in a desert that had not been subject to O&M for 3 months was 0.26–0.30 mm. Hence, in this study, the maximum surface roughness height and area were limited to 0.3 mm and 50%, respectively.

To define the erosion shape for CFD simulation, the state of erosion at the leading edge of a Vestas V47 blade that has been in operation for 12 years without any O&M activity was examined (Fig. 2). Erosion was found only on the pressure side in sections where the radial distance from the hub was less than 85% of the blade length, whereas erosion expanded to the suction side in sections where the radial distance from the hub was more than 85% of the blade length, causing the most critical delamination damage at the tip end. Surface erosion gradually expanded from the pressure side near the stagnation point to the suction side, and the depth and width of the erosion increased in sections closer to the tip. In this study, the state of erosion at the leading edge of a NACA64-618 airfoil was classified as follows. The depth and width of the erosion was calculated by referring to the state of erosion at cross-sections at which the radial distance to the blade was 85%, 90%, and 95% of the blade length, respectively. Nine conditions of contamination were thus defined: roughness height of 0.1, 0.2, and 0.3 mm, each with roughness areas of 10%, 30%, and 50%. Accordingly, three conditions of erosion were defined: erosion depth of 3.4, 3.6, and 4.8 mm (light, moderate, and heavy erosion, respectively), with respective erosion widths of 10, 17.4, and 37 mm (Table 2).

## 3. Effect of Contamination and Erosion Conditions on the Aerodynamic Performance of Airfoils

### *3.1 Numerical setup*

The commercial CFD software Star-CCM+ version 10.04 was used to estimate the variation in the aerodynamic performance of airfoils at different levels of contaminant accumulation and erosion. An irregular vortex was expected to be generated from the suction side of the airfoil in sections where the angle of attack was higher than a threshold, leading to a stall. The time to the generation of such a vortex might vary substantially because of surface roughness variation and erosion, which disrupt the fluid flow of the leading edge. Hence, transient simulation was performed.

Total simulation time was set as 0.8 s, with time steps of 0.0005 s. Convergence was defined as a RMS residual value lower than $10^{-4}$ with stable lift and drag coefficients.

The computational mesh and boundary condition are as described in Fig. 3. The inlet boundary condition was established as the velocity inlet. The inflow wind speed was set as 89.6326 m/s, which corresponds to a flow with a Reynolds number of 6 × E06, and turbulence intensity was set as 0.01%. The environmental pressure outlet condition was applied as the outlet boundary condition. The distance from the airfoil to the inlet boundary surface was 20 times the chord length, and that from the airfoil to the outlet boundary surface was 40 times the chord length, both of which ensure a sufficient flow domain. A hexa-type mesh was used to enhance convergence and reliability of the calculation. The y+ [12] was set such that it satisfied the recommended values for the given characteristics of the turbulence model. Shear stress transport (SST) k–ω and SST k–ω transition models fulfill the condition of $y+ < 1$, and the k–ε model fulfills the condition of $y+ > 30$.

Star-CCM+ provides various turbulence models, such as realizable k–ε, SST K–ω, and SST K–ω transition ($\gamma - \theta$) models. The k–ε turbulence model, the most widely used in engineering simulations, has high accuracy in estimating flows in free stream, but it overestimates turbulence shear stress when an adverse pressure gradient exists in the boundary layer. Hence, the flow separation point in models with a curvature, such as in the case of airfoils, cannot be accurately estimated. By contrast, the SST k–ω model combines the advantages of the Wilcox model, which estimates near-wall flow with high accuracy, and the K–ε model used for free stream flows. This model can estimate the flow separation point and the size of the vortex with high precision.

Fully turbulent flow fields are assumed in the realizable k–ε and SST K–ω models. Hence, they cannot accurately reflect the flow of the boundary layer near the leading edge of an airfoil, where laminar, transition, and turbulent flows exist simultaneously. Thus, in this study, a turbulence model that most reliably analyzes aerodynamic performance, determined through turbulence dependency tests, and an SST K–ω transition ($\gamma - \theta$) model, a correlation-based transitional turbulence model, were used.

Table 3 lists the results of the mesh dependency test for an angle of attack of 8° and Reynolds number of 6 × E06. Three cases—cases 1–3 with 200,000, 250,000, and 300,000 mesh nodes, respectively—were established in the flow domain except in the area near the wall, where the number of meshes was adjusted to ensure comparable mesh quality. A relative error was found for Case 1, whereas relative errors were unlikely in Cases 2 and 3. Therefore, 250,000 meshes were used in this study

In Fig. 4, the results of the turbulence dependency test are compared with the wind tunnel test results reported by Abbott et al. [13]. Except for the lift–drag ratios in sections where the angle of attack is 4°, the results of the SST K–ω transition turbulence model were similar to those of the wind tunnel test for most angles of attack. In particular, fully turbulent models underestimate drag, thereby leading to significantly high relative errors in the lift–drag ratios. Hence, the SST k–ω transition was used as the turbulence model in this study.

### *3.2 Equivalent sand-grain roughness*

In most commercial CFD codes, equivalent sand-grain roughness (ESGR) is used for modeling a rough

wall. Nikuradee et al. first proposed an ESGR estimation equation by experimentally investigating internal flow in pipes, but this equation could not account for the shape and surface roughness distribution; hence, Sigal et al. [14-15] revised the ESGR estimation equation:

$$\Lambda_s = \left(\frac{S}{S_f}\right)\left(\frac{A_f}{A_s}\right)^{-1.6} \quad \text{Eq.(1)}$$

$$\frac{K_s}{K} = \begin{cases} 0.003215\Lambda_s^{4.925} & 1.4 \le \Lambda_s \le 4.89 \\ 8.0 & 4.89 \le \Lambda_s \le 13.25 \\ 151.71\Lambda_s^{-1.1379} & 13.25 \le \Lambda_s \le 100.0 \end{cases} \quad \text{Eq.(2)}$$

where $K_s$ is the ESGR, K is the roughness element height, and $\Lambda_s$ is a roughness parameter. S is the reference area (i.e., the area of the corresponding smooth surface without any roughness), $S_f$ is the total frontal area of the rough surface, $A_f$ is the frontal area of a single roughness element, and $A_s$ is the surface area of a single roughness element in the direction of wind flow. $S/S_f$ and $A_f/A_s$ are density and shape parameters, respectively.

To calculate the ESGR by using the aforementioned equation, $S/S_f$, $A_f/A_s$, and K should be determined. To obtain reliable ERGS, the CFD simulations were executed using the same conditions as those applied in the wind tunnel test conducted by Timmer et al, and the aforementioned parameters were determined by comparing the simulations and the experimental results. Timmer et al. simulated surface roughness by placing 0.28-mm carborundum grains (grit number 60) in an area accounting for 8% of the chord length from the leading edge of the airfoil. Hence, in this study, the height of the carborundum grains was set as the K, and the shape parameter was set as 1 under the assumption that the roughness element shape is a square (Fig. 5). The same condition S (8%) as that used in the wind tunnel test was set at the leading edge of the airfoil, and ESGR for various $S_f$ is listed in Table 4.

The CFD simulation results under the aforementioned conditions are summarized in Table 5. The lift–drag ratios, a main index for the aerodynamic performance of airfoils, indicate that over the complete range of angles of attack, the CFD simulation for an $S_f$ of 2.64% is the most consistent with the wind tunnel test results. Therefore, in this study, the ESGR for use in the CFD simulations conducted to evaluate the effect of contamination on power performance was calculated by using $S_f$ of 2.64% as well as the various roughness height conditions listed in Table 2. In CFD simulations conducted to evaluate the effect of erosion on power performance, the ESGR calculated at a K of 0.3 mm was used.

### *3.3 CFD simulations*

Unsteady flow analysis on sections subject to an angle of attack of −5° to 16° was conducted through CFD simulation. The lift coefficient decreased significantly, relative to that of a clean airfoil, in Case 9 (height of contaminant accumulation: 0.3 mm; contamination area: 50%) and Case 12 (erosion condition: heavy); these two cases reflect the most critical contamination and erosion conditions at the leading edge

(Fig. 6). Further, aerodynamic performance decreased significantly at angles of attack of 6° and more. The stall point varied with the conditions of leading edge—14° in the clean airfoil and 12° and 8°, respectively, in Cases 9 and 12—because flow separation occurs earlier as the extent of surface roughness increases. In addition, a deep stall can occur in cases of extreme damage.

The simulated changes in the aerodynamic performance of the leading edge with variation in the contamination and erosion conditions are presented in Tables 6 and 7, respectively. Increase and decrease in the lift and drag coefficients, relative to those of the corresponding clean airfoil, are represented by + and −, respectively. Under a given contamination condition, aerodynamic performance decreases as the height and area of the contaminant accumulation increase. Moreover, lift coefficient decreases by up to 34%, and the drag coefficient increases by up to 159%. With aggravation of the erosion conditions, aerodynamic performance decreases further, lift coefficient decreases by up to 53%, and the drag coefficient increases by up to 314%. These results reveal that aerodynamic performance is affected more severely by erosion than by contamination.

## 4. Effect of Contamination and Erosion on AEP

### *4.1 AEP calculation*

For calculating AEP losses, numerical modeling of a 5-MW NREL wind turbine, the reference wind turbine system, was conducted using the integrated load calculation software BLADED (DNV). Each blade of this turbine is composed of cylinder and following airfoils[16]: Cylinder (r/R = 2%), DU99-W-405 (r/R = 18.7%), DU99-W-350 (r/R = 25.2%), DU97-W-300 (r/R = 38.2%), DU91-W2-250 (r/R = 44.7%), DU91-W-210 (r/R = 57.7%), and NACA 64-618 (r/R = 70.7%).

The power and load of the wind turbine under various operational conditions can be obtained when the aerodynamic data of each section for angles of attack ranging from **−180° to 180°** are input into the software. Therefore, the required aerodynamic data for this wide range were obtained by extrapolating the CFD simulation results obtained over for angles of attack of −5° to 16°, according to the method proposed by Snel et al. [17].

Aerodynamic data of clean airfoils in sections located at up to 70.7% of the blade radius from the blade root were obtained from the reference data [10], and the simulated aerodynamic data under various contamination and erosion conditions were for sections containing NACA 64-618 airfoils farther than 70.7%.

The steady power calculation was performed using BLADED to obtain the steady power curve required for AEP calculation of wind turbines. Figure 7 presents the power curve of clean airfoil and lightly and heavily eroded airfoils. Because of the aggravated surface damage at the tip of the airfoil, the condition to reach the rated wind speed is prolonged, leading to low power output at lower-than-rated wind speeds. At higher-than-rated wind speeds, the pitch control ensures that the rated output power is maintained.

The Weibull probability density function was applied to calculate the AEP of the reference wind

turbine. The frequency of occurrence f(V) of each wind speed was derived using Eq. (3), and the scale parameter(c) was evaluated by Eq. (4), where Γ is the gamma function.[18-19]

Subsequently, the AEP was calculated using Eq. (5), where P(V) is the output power for each wind speed and 8760 is hours in a year; the following conditions were assumed: air density = 1.225 kg/m³, shape parameter (k) = 2, mean wind speed = 8 m/s, and availability = 100%.

$$f(V) = \frac{k}{c}\left(\frac{V}{c}\right)^{k-1}\exp\left[-\left(\frac{V}{c}\right)^{k}\right] \quad \text{Eq. (3)}$$

$$\overline{V} = c\Gamma\left(1+\frac{1}{k}\right) \quad \text{Eq. (4)}$$

$$AEP = 8760 \times \int_{cut-in}^{cut-out}[P(V)\times f(V)]dV \quad \text{Eq. (5)}$$

***4.2 Calculated AEP***

AEP losses under various conditions of blade contamination and erosion and lift–drag ratios of airfoils at cross-sections (r/R = 70.7%) of a blade are shown in Fig. 8. AEP losses were separately calculated for sections subject to wind speeds lower and higher than the rated wind speed and summed to obtain the total AEP loss. In sections subject to higher-than-rated wind speeds, the effects of blade pitch control restricted the maximum AEP loss to 0.01 GWh, whereas sections subject to lower-than-rated wind speeds had significant AEP losses of 0.36–0.67 GWh.

AEP losses are closely related to the control system of the wind turbine. The variable speed–variable pitch control of the reference wind turbine controls the generator torque and the blade pitch angle when the wind speed is lower or higher than the rated wind speed, respectively. Thus, as the aerodynamic performance of the blades deteriorate at lower-than-rated wind speeds, the rotational speed of the generator decreases, leading to significant power losses.

Changes in the pitch angle at higher-than-rated wind speeds under clean and erosion conditions (light and heavy) are depicted in Fig. 9. Data in the figure confirm that the aerodynamic performance of highly damaged blade tip areas can be partially restored by finely adjusting the pitch angle such that the AEP losses are minimized.

The angle of attack in the blade tip area (r/R > 70.7%) at lower-than-rated wind speeds ranges from 2.68° to 7.59°. The decrease in the lift–drag ratio at wind speeds of 4–12 m/s (Fig. 8) illustrates the correlation between aerodynamic performance and AEP loss in these sections. For contaminated blades, the minimum and maximum reduction in the lift–drag ratio was 40% (Case 1) and 67.4% (Case 9), respectively; in both these cases, the wind speed was 4 m/s. Overall, AEP losses were between 0.41 GWh (Case 1) and 0.68 GWh (Case 9). For eroded blades, the minimum and maximum reduction in the lift–

drag ratio was 35.4% (Case 10) and 66.4% (Case 12), respectively; in both these cases, the wind speed was 4 m/s. Overall, AEP losses were between 0.36 GWh (Case 10) and 0.65 GWh (Case 12). As described in Section 3.4, aerodynamic performance is more severely affected by erosion, but the AEP losses under erosion conditions are similar to those under contamination conditions; this is because the change in the angle of attack at the blade tip area in sections subject to lower-than-rated wind speeds is relatively narrow. The reduction in aerodynamic performance under the investigated conditions was the most significant at an angle of attack of 10° and higher. Nevertheless, these angles of attack occur at higher-than-rated wind speeds, where the blade pitch control likely prevents AEP losses.

## 5. Conclusions

The effects of contamination and erosion at the leading edge of blades on the AEP of wind turbines were quantitatively analyzed. The pertinent aerodynamic data were obtained through transient CFD simulations of NACA 64-618 airfoils, and the corresponding AEP losses were calculated by applying these data to the tip area of the 5-MW NREL reference wind turbine model.

For blades with contaminant accumulation at the leading edge of the airfoil, the lift and drag coefficients decreased by up to 27% and 159%, respectively, compared with those of a clean airfoil. For blades subject to erosion at the leading edge, the lift and drag coefficients decreased and increased by up to 53% and 314%, respectively. Reduction in the aerodynamic performance tended to increase with the extent of surface damage at the leading edge of the airfoil, especially in the section exposed to large angles of attack (10° and higher).

The maximum AEP loss under contaminant accumulation conditions was 0.68 GWh and that under erosion conditions was 0.65 GWh. The trend of AEP loss was consistent with that of the reduction in the lift–drag ratio. Overall, the calculated AEP loss ranged from 2% to 3.7% depending on the extent of damage at the leading edge.

**Acknowledgements**

This study was supported by “Development for image inspection and cleaning system of Wind turbine blade surface” and “Human Resources Program in Energy Technology” of the Korea Institute of Energy Technology Evaluation and Planning(KETEP), granted financial resources from the Ministry of Trade, Industry & Energy, Republic of Korea (Grant Nos. 20153030023750 and 20164030201230)

## References


[1] N. Dalili, A Edrsy, R Carriveau, A review of surface engineering issues critical to wind turbine performance, renewable and sustainable energy, November 7, 2007.

[2] Eduardo Garcia Perez, Wind farm owner's view on rotor blades from O&M to design requirements, International Conference Wind Turbines Rotor Blade O&M, 2014.

[3] Agrim Sareen, Chimay A. Sapre and Michael S. Selig, Effects of leading edge erosion on wind turbine blade performance, Wind Energy2014.

[4] Mohammed G. Khalfallah, Aboelyazied M. Koliub, Effect of dust on the performance of wind turbines, Desalination, Vol. 209, No, 1-3, pp.209-220, April30, 2007.

[5] Corten GP, Veldkamp HF, Insects cause double stall. Copenhagen : EWEC, 2001.

[6] Corten GP, Veldkamp HF, Insects can halve wind-turbine power. Published in Nature, Vol. 412; 42-43, 5 July 2001.

[7] C. J. Spruce, Power performance of active stall wind turbines with blade contamination, Conference proceedings of EWEC 2006.

[8] Deshun Li, Rennian Li, Congxin Yang & Xiuyong Wang, Effects of Surface Roughness on Aerodynamic Performance of a Wind Turbine Airfoil, IEEE, 2010.

[9] Nianxin Ren, Jinping Ou, Dust effect on the performacne of Wind Turbine Airfoils. J. Electromagnetic Analysis & Applications, 1: 102 -107, 2009.

[10] J Jonkman, S Butterfield, W Musial and G Scott, Definition of a 5 MW reference wind turbine for offshore wind system development, National Renewable Energy Laboratory, Golden, CO, USA, 2006.

[11] Michael F. Kerho, Michael B. bragg, Airfoil Boundary-Layer Development and Transition with Lare Leading-Edge Roughness, AIAA Journal vol. 35, No. 1, January 1997.

[12] Mohd ARIFF, Salim M. SALIM and Siew Cheong CHEAH, Wall Y+ Approach for Dealing with Turbulent Flow over a Surface Mounted Cube: Part 1 – Low Reynolds Number, International conference on CFD in the Minerals and process Industries, pp.9-11 December 2009.

[13] IRA H., Abbott, Albert E. von Doenhoff and Louis S. Stivers Jr, Summary of Airfoil Data - Report No. 824, National Advisory Committee for Aeronautics, pp.195. 1945.

[14] Sigal,A., and Danberg, J E, Analysis of Turbulent Boundary Layer Over Rough Surfaces With Application to Projectile Aerodynamics, Army Ballistic Research Lab, Aberdeen Proing Grounds MD, Technical Report BRL-TR-2977, 1988.

[15] Qiang zhang, Sang Woo Lee, Phillip M. Ligrani, Effects of Surface Roughness and Turbulence Intensity on the Aerodynamic Losses Prdouced by the Suction surface of a simulated Turbine airfoil, Journal of Fluids Engineering, Vol 126, March 2004.

[16] Brian R. Resor, Definition of a 5MW/61.5m Wind Turbine Blade Reference Model, Sandia Report

SAND2014-2569, pp.15, April 2013.

[17] Snel, H., Houwink, R. and Piers, W. J, Sectional Prediction of 3D Effects for Seperated Flow on Rotating Blade, 18th European Rotorcraft Forum, 1992.

[18] I. kwon, J. Kim, I. Paek and N. Yoo, Variation of capacity factors by weibull shape parameters, Journal of the Korean Solar Energy Society, Vol. 33, No.1, 2013.

[19] Paritosh BHATTACHARYA and Rakhi BHATTCHARJEE, A Study on Weibull Distribution for Estimating the Parameters, Journal of Applied Quantitative Methods, Vol. 5, No.2, Summer 2010

# Figures

Fig. 1 Contamination and erosion at the leading edge of wind turbine blades

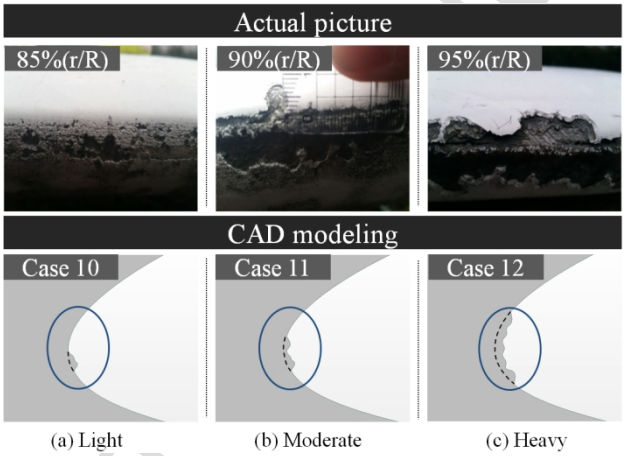


Fig. 2 Erosion conditions at the leading edge of a 12-year-old Vestas V47 blade

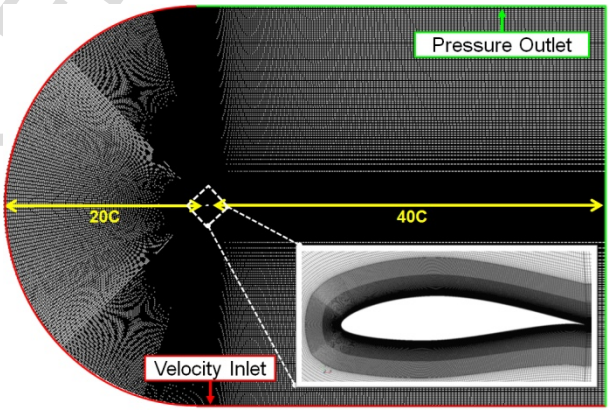


Fig. 3 Boundary conditions used in the CFD simulation

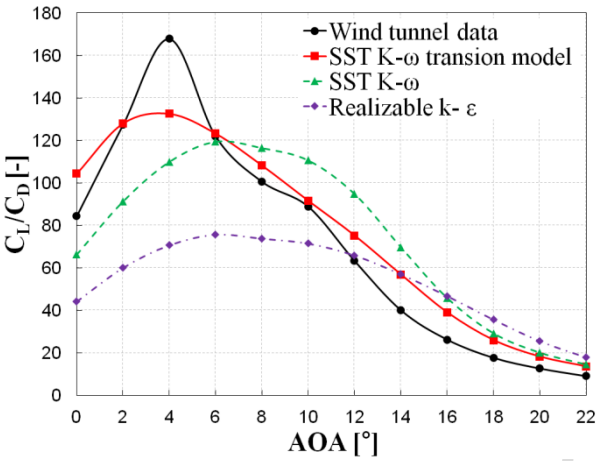


Fig. 4 Lift–drag ratios in various turbulence models

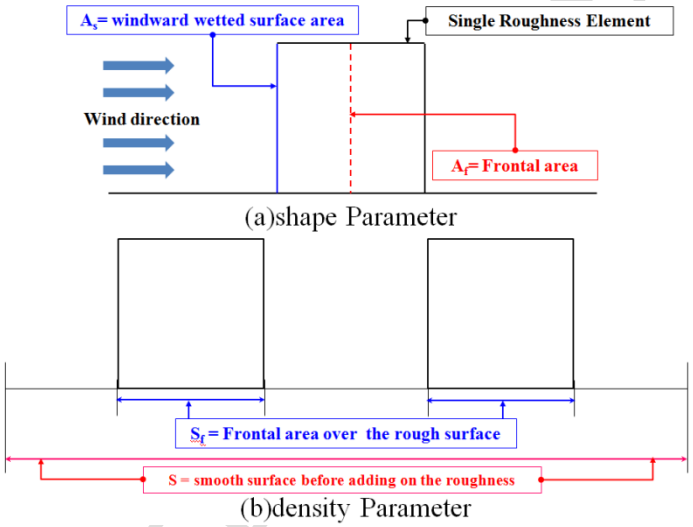


Fig. 5 Shape and density parameters used for calculating the ESGR

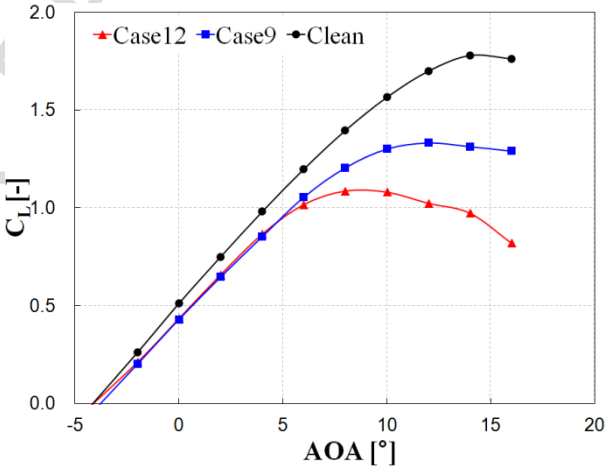


Fig. 6 Variation in lift coefficients with surface conditions of the blade (Clean, Case 9, Case 12)

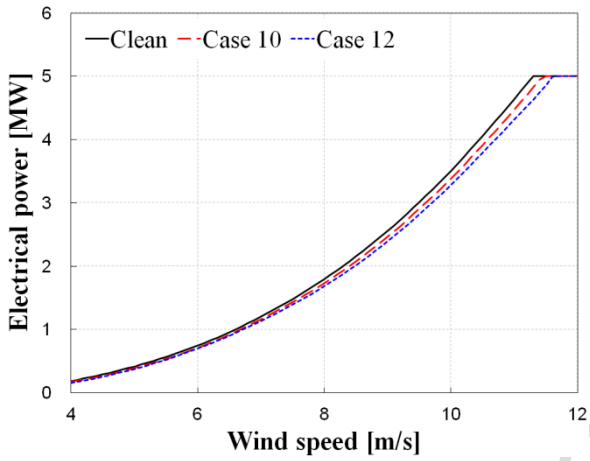


Fig. 7 Effects of surface erosion conditions on output power (Clean, Case 10, Case 12)

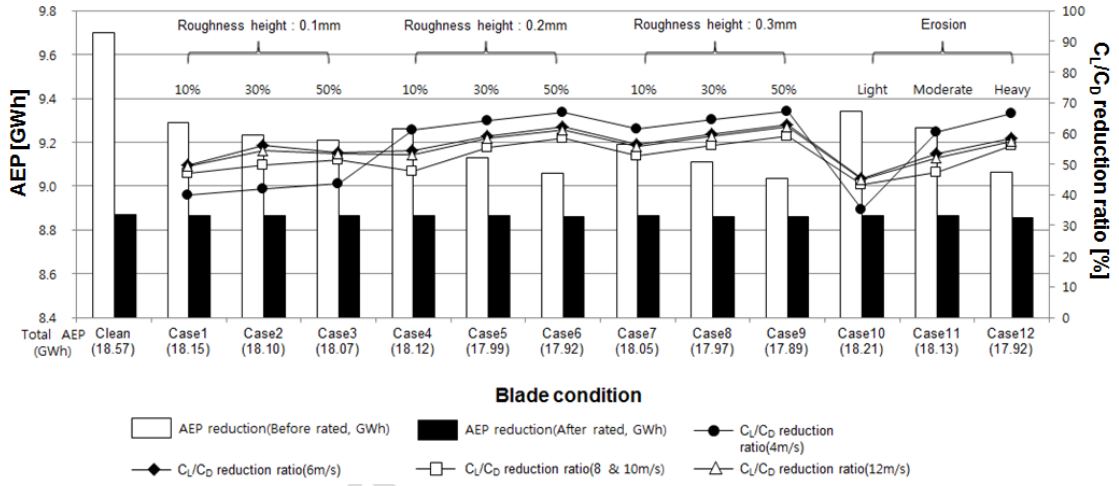


Fig. 8 AEP loss and lift–drag ratios under various blade surface conditions

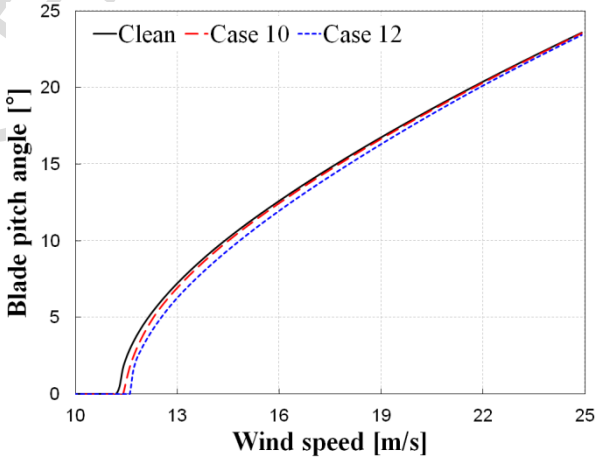


Fig. 9 Effects of surface erosion conditions on pitch angle (Clean, Case 10, Case 12)

# Tables

Table 1. Specifications of the NREL 5-MW wind turbine

| | |
|---|---|
| Rating | 5 MW |
| Rotor orientation | Upwind |
| Control | Variable speed variable pitch |
| Rotor, hub diameter | 126 m, 3 m |
| Cut-in, rated, cut-out wind speeds | 4 m/s, 11.4 m/s, 25.4 m/s |
| Rated rotor speed | 12.1 rpm |
| RNA mass | 350,000 kg |
| Tower mass | 347,460 kg |

Table 2. Contamination and erosion conditions

Contamination conditions

| Case | Roughness area [%] | Roughness height [%] |
|---|---|---|
| 1 | 10 | 0.1 |
| 2 | 30 | |
| 3 | 50 | |
| 4 | 10 | 0.2 |
| 5 | 30 | |
| 6 | 50 | |
| 7 | 10 | 0.3 |
| 8 | 30 | |
| 9 | 50 | |

Erosion Conditions

| Case | State | Depth [mm] | Width [mm] |
|---|---|---|---|
| 10 | Ligth | 3.4 | 10.0 |
| 11 | Moderate | 3.6 | 17.4 |
| 12 | Heavy | 4.8 | 37.0 |

Table 3 Results of the mesh dependency analysis

| Case | AoA (°) | Mesh No. | $C_l$ | $C_d$ |
|---|---|---|---|---|
| 1 | 8 | 200000 | 1.373 | 0.0143 |
| 2 | | 250000 | 1.396 | 0.0129 |
| 3 | | 300000 | 1.4 | 0.0130 |

Table 4 ESGR for various $S_f$

| Roughness element heigth [mm] | $A_f/A_s$ | $S_f$[%] | ESGR |
|---|---|---|---|
| 0.28 | 1 | 3.36 | 0.067 |
| | | 3.04 | 0.100 |
| | | 2.88 | 0.143 |
| | | 2.64 | 0.200 |
| | | 2.48 | 0.270 |

Table 5 Results of the wind tunnel test and CFD simulations for various $S_f$

| AoA(°) | CFD simulation | | | | | | Wind tunnel | |
|---|---|---|---|---|---|---|---|---|
| | rough | | | | | Clean | Clean | rough |
| | $S_f$ (=3.36) | $S_f$ (=3.04) | $S_f$ (=2.88) | $S_f$ (=2.64) | $S_f$ (=2.48) | | | |
| | Cl/Cd | Cl/Cd | Cl/Cd | Cl/Cd | Cl/Cd | Cl/Cd | Cl/Cd | Cl/Cd |
| 0 | 82.94 | 81.51 | 62.85 | 40.22 | 39.85 | 104.31 | 84.35 | 38.89 |
| 2 | 95.63 | 115.94 | 62 | 53.12 | 94.89 | 127.98 | 127.37 | 54.27 |
| 4 | 70.07 | 69.29 | 68.52 | 61.77 | 60.85 | 132.56 | 167.85 | 60.36 |
| 6 | 70.48 | 69.65 | 68.98 | 67.91 | 62.25 | 123.25 | 121.98 | 59.86 |
| 8 | 65.24 | 64.21 | 63.43 | 62.63 | 60.14 | 108.22 | 100.63 | 49.17 |

Table 6 Relative error of the drag coefficients under various contamination and erosion conditions at the leading edge of airfoils

| AoA (°) | Contamination Cases [%] | | | | | | | | | Erosion Cases [%] | | |
|---|---|---|---|---|---|---|---|---|---|---|---|---|
| | 1 | 2 | 3 | 4 | 5 | 6 | 7 | 8 | 9 | 10 | 11 | 12 |
| −5 | 45 | 48 | 52 | 48 | 55 | 65 | 87 | 98 | 111 | 44 | 61 | 145 |
| −2 | 65 | 67 | 73 | 124 | 137 | 152 | 125 | 140 | 157 | 57 | 67 | 145 |
| 0 | 57 | 60 | 67 | 126 | 140 | 155 | 130 | 142 | 159 | 48 | 121 | 156 |
| 2 | 85 | 92 | 98 | 111 | 124 | 138 | 112 | 126 | 141 | 82 | 106 | 120 |
| 4 | 74 | 81 | 86 | 76 | 104 | 115 | 93 | 106 | 119 | 65 | 74 | 99 |
| 6 | 62 | 69 | 74 | 64 | 94 | 82 | 67 | 77 | 87 | 53 | 68 | 109 |
| 8 | 55 | 62 | 67 | 57 | 68 | 76 | 61 | 72 | 82 | 47 | 72 | 140 |
| 10 | 56 | 64 | 69 | 60 | 72 | 80 | 65 | 77 | 88 | 49 | 93 | 188 |
| 12 | 67 | 75 | 81 | 73 | 84 | 96 | 77 | 91 | 105 | 63 | 126 | 225 |
| 14 | 74 | 79 | 86 | 79 | 88 | 101 | 85 | 96 | 110 | 73 | 151 | 247 |
| 16 | 80 | 83 | 88 | 85 | 92 | 100 | 91 | 99 | 107 | 83 | 155 | 314 |

Table 7 Relative error of the lift coefficients under various contamination and erosion conditions at the leading edge of airfoils

| AoA (°) | Contamination Cases [%] | | | | | | | | | Erosion Cases [%] | | |
|---|---|---|---|---|---|---|---|---|---|---|---|---|
| | 1 | 2 | 3 | 4 | 5 | 6 | 7 | 8 | 9 | 10 | 11 | 12 |
| −5 | 3 | 3 | 3 | 3 | 3 | 6 | 29 | 31 | 34 | −1 | −1 | −18 |
| −2 | −5 | −5 | −5 | −19 | −20 | −22 | −19 | −21 | −23 | −3 | −5 | −19 |
| 0 | −4 | −4 | −5 | −13 | −14 | −16 | −14 | −15 | −16 | −3 | −13 | −15 |
| 2 | −10 | −12 | −11 | −11 | −12 | −13 | −11 | −13 | −14 | −2 | −11 | −12 |
| 4 | −9 | −10 | −10 | −9 | −12 | −13 | −10 | −12 | −13 | −8 | −9 | −12 |
| 6 | −9 | −10 | −10 | −9 | −10 | −11 | −9 | −11 | −12 | −8 | −10 | −15 |
| 8 | −10 | −11 | −11 | −10 | −12 | −13 | −11 | −12 | −14 | −8 | −12 | −22 |
| 10 | −11 | −13 | −14 | −12 | −14 | −16 | −13 | −15 | −17 | −10 | −18 | −31 |
| 12 | −15 | −16 | −17 | −16 | −18 | −20 | −17 | −19 | −22 | −14 | −25 | −40 |
| 14 | −19 | −20 | −21 | −20 | −22 | −24 | −21 | −23 | −26 | −19 | −32 | −45 |
| 16 | −20 | −21 | −23 | −22 | −23 | −25 | −23 | −25 | −27 | −21 | −35 | −53 |